Proc. Nat. Acad. Sci. USA
Vol. 71, No. 6, pp. 2478–2481, June 1974

Further Analysis of a Simple Prototypal Muscle Model Near to and Far from Equilibrium

(sliding filament model/isotonic contractions/efficiency/irreversible thermodynamics)

TERRELL L. HILL AND YI-DER CHEN

Laboratory of Molecular Biology, National Institute of Arthritis, Metabolism, and Digestive Diseases, National Institutes of Health, Bethesda, Maryland 20014

Contributed by Terrell L. Hill, April 8, 1974

ABSTRACT **The same prototypal model used in a previous paper to illustrate proper construction of a muscle model is modified here with the much more realistic choice $e^{\Delta_p} = 10^8$ rather than $e^{\Delta_p} = 100$, where e^{Δ_p} is the ratio of physiological ATP activity to equilibrium ATP activity. For steady isotonic contractions, the range $1 \leqslant e^{\Delta} \leqslant 10^4$ can be approximated quite well by use of linear terms only in expansions of $\bar{F}$ (force) and $\bar{J}$ (ATP flux) in powers of $e^{\Delta} - 1$ and v (velocity). This will presumably also be true in most cases of much more complicated models. However, this region is of theoretical interest only (irreversible thermodynamics, etc.) because $\bar{F}$ and $\bar{J}$ are very small. In addition, numerical calculations of $\bar{F}$ and $\bar{J}$ were made in the region $10^4 \leqslant e^{\Delta} \leqslant 10^8$. The optimal efficiency η^* is larger under physiological conditions (about 1%) than at equilibrium by a factor of 2.1×10^4. The rate of entropy production is discussed in this connection.**

This work is a continuation of an earlier paper (1) with essentially the same title. Availability of the previous paper to the reader is assumed. In both of these papers, our object is to illustrate the proper formulation and use of a complete and self-consistent molecular model of muscle. Otherwise, the model employed is *not* meant to be a practical muscle model.

In the first set of calculations (1), we used, arbitrarily, $e^{\Delta_p} = 100$ for the "physiological" value of $\Delta = (\mu_T - \mu_T^e)/kT$ and investigated, primarily, the range $e^{\Delta} = 100$ to $e^{\Delta} = 1$ (equilibrium). Note that e^{Δ} is proportional to ATP activity (or concentration). This relatively small range in e^{Δ} had the pedagogical advantage of preserving a certain degree of continuity between the two ends of the range. But the *actual* physiological value of e^{Δ} is of order 10^8. Therefore, in this paper, we take $e^{\Delta_p} = 10^8$ as the physiological value and study the much wider range in ATP activity (or concentration), $e^{\Delta} = 10^8$ to $e^{\Delta} = 1$, using the same model as before (1) except for modifications required by the change in the value of Δ_p. To a considerable extent, the results can be divided into two regimes: $10^4 \leqslant e^{\Delta} \leqslant 10^8$ and $1 \leqslant e^{\Delta} \leqslant 10^4$. The latter regime is of theoretical interest only.

The model

The two-state cycle is shown in Fig. 1. We use the dimensionless notation already introduced (1). The rate constants $f(x)$ and f' are unaltered (as are also the free energy functions):

$$f(x) = 3e^{-x^2/2}, \qquad f' = 0.17833. \qquad [1]$$

But for $g(x)$ we use

$$g(x) = g^e(x)e^{\Delta} \qquad [2]$$

where

$$g^e(x) = (0.15 + e^{-1.5x}) \times 10^{-8}. \qquad [3]$$

Thus, the function $g(x)$ under physiological conditions ($\Delta = \Delta_p$) is unchanged, as is clear on comparing Fig. 2 here with Fig. 2 in ref. 1. But $g^e(x)$ is reduced in magnitude here by a factor of 10^6. Since $f'g'(x) = f(x)g^e(x)$, the function $g'(x)$ is also reduced by a factor of 10^6:

$$\begin{aligned} g'(x) &= f(x)g^e(x)/f' \\ &= 0.16823 \times 10^{-6}\, e^{-x^2/2}\,(0.15 + e^{-1.5x}). \end{aligned} \qquad [4]$$

Hence, on the scale of Fig. 2, $g'(x)$ is essentially zero. [But we use Eq. **4** for $g'(x)$ in the computer program.] This virtual elimination of $g'(x)$ is the only change in the model, compared to the previous case (1), *under physiological conditions*. This is not a drastic change, since $g'(x)$ in ref. 1 is already not very large. But at equilibrium, both of the g and g' processes (involving adsorption and desorption of ATP, respectively) are almost missing (Eqs. **3** and **4**), as they should be in "real" models. This produces drastic effects on properties of the system "near" equilibrium (see below).

In both examples ($e^{\Delta_p} = 100$ and 10^8) we have used $g \sim e^{\Delta}$ over the whole concentration range of ATP. However, this is not the only possibility (see Appendix II of ref. 2). Because the diagram has been reduced to two effective states, other examples would be possible in which there is a Langmuir-isotherm type of dependence of g on e^{Δ} and a related (by detailed balance) dependence of g' on e^{Δ} (2).

Steady isometric contractions

Fig. 3 shows the calculated curves $\bar{F}_0(\Delta)$ and $\bar{J}_0(\Delta)$ for $e^{\Delta} > 10^4$. On the *left* of the figure are the same curves taken from ref. 1 ($e^{\Delta_p} = 100$). The *arrows* on the abscissa indicate physiological values. Using the present more realistic and extensive range in Δ, it is seen that, as the ATP activity is decreased, $\bar{F}_0$ and $\bar{J}_0$ have become practically zero when the physiological ATP activity has been reduced by a factor of about 10^4 for $\bar{F}_0$ and about 10^3 for $\bar{J}_0$. For *practical* purposes, further reduction of the ATP activity to $e^{\Delta} = 1$ (equilibrium) is of little consequence. Because of the unrealistic small range in e^{Δ}, this kind of two-stage behavior in $\bar{F}_0$ and $\bar{J}_0$ does not occur in the $e^{\Delta_p} = 100$ case.

The *dashed* $\bar{F}_0$ *curve* in Fig. 3 refers to a different and simple model for which an analytical expression for $\bar{F}_0(\Delta)$ can be

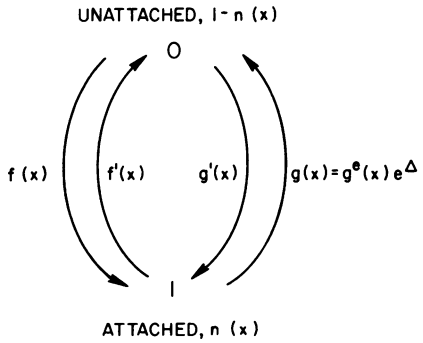

FIG. 1. Two-state diagram used in calculations.

derived (see the *Appendix*). The value $e^{\Delta_p} = 10^8$ is also used in this case.

To show the full range in e^{Δ}, the $e^{\Delta_p} = 10^8$ curves in Fig. 3 are replotted in Fig. 4 using a logarithmic ordinate. Near the origin, all curves are heading for negative infinity since $\bar{F}_0 = 0$ and $J_0 = 0$ at equilibrium ($e^{\Delta} = 1$). The *dotted curves* labeled "linear" will be discussed below.

Steady isotonic contractions

By solving the appropriate differential equation, Eq. 3 of ref. 1, we have calculated $\bar{F}$ and $\bar{J}$ at $e^{\Delta} = 10^8$, 1.5×10^7, 1.1×10^6 and 10^4, for several values of v in each case. Fig. 5 shows $\bar{F}(v)$ and $\bar{J}(v)$ for the first three values of e^{Δ}. These curves are approximately linear in the case $e^{\Delta} = 1.1 \times 10^6$, and they are very close to linear in the case $e^{\Delta} = 10^4$ (not shown).

Using the above results, we estimate, by interpolation, that the optimal efficiency is $\eta^* = 0.0085$, 0.0095, 0.0068, and 0.000415 for the four respective values of e^{Δ} listed above. These points, together with the corresponding estimates of v^*, are included in Fig. 6. The extension of the functions log η^* and log v^* to $e^{\Delta} = 1$, and the curves labeled "linear," are discussed below. Note that η^* increases, at first, for greater departures from equilibrium, and passes through a maximum of about 0.95% at about $e^{\Delta} = 1.5 \times 10^7$. The physiological efficiency (0.85%) is less here than in the previous case (3.1%) primarily because Δ_p is larger (recall that $\eta = \bar{F}v/J\Delta$). Incidentally, as already mentioned (1), we have found self-consistent and rather realistic two-state models with efficiencies very much larger (above 30%) than in these examples (unpublished work with E. Eisenberg and R. Podolsky).

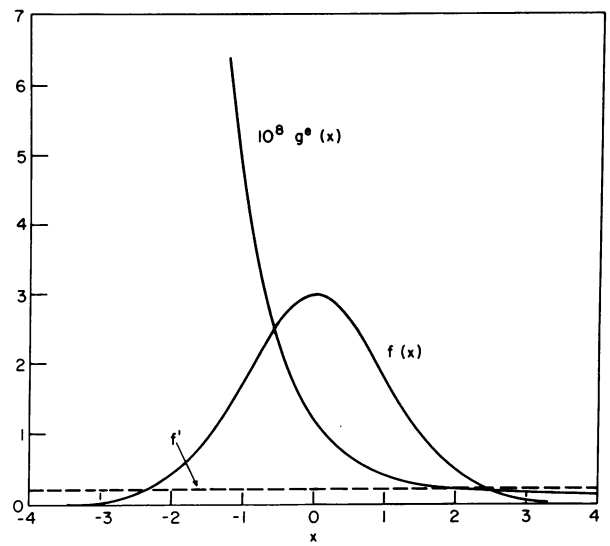

FIG. 2. Rate constant functions used in calculations ($e^{\Delta_p} = 10^8$). The function $g'(x)$ is not apparent on this scale.

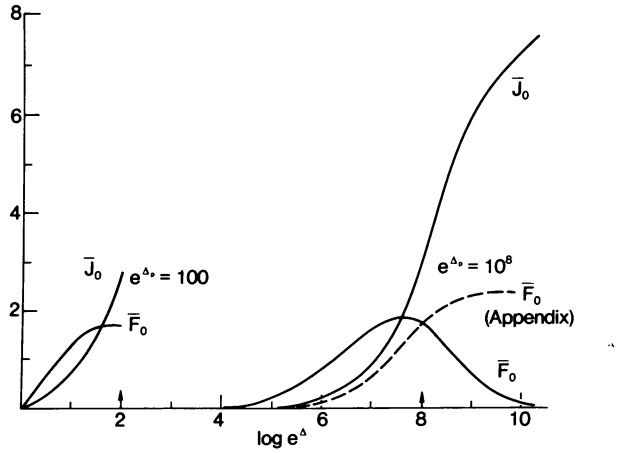

FIG. 3. *Right side:* isometric force and flux in the case (present paper) $e^{\Delta_p} = 10^8$ (see the *Appendix* concerning the *dashed curve*). *Left side:* isometric force and flux in the case (ref. 1) $e^{\Delta_p} = 100$.

Steady isotonic contractions "near" equilibrium

We showed in the previous paper (1) how to find the beginning coefficients in expansions of $\bar{F}$ and $\bar{J}$ in powers of Δ and v. Linear and quadratic coefficients were actually calculated. Alternatively, one can expand $\bar{F}$ and $\bar{J}$ in powers of $e^{\Delta} - 1$ and v. In fact, if we have found the coefficients in

$$\begin{aligned} \bar{F} &= A\Delta - Bv + c'_{11}\Delta^2 + c_{12}v\Delta + c_{22}v^2 + \cdots \\ J &= C\Delta + Av + d'_{11}\Delta^2 + d_{12}v\Delta + d_{22}v^2 + \cdots \end{aligned} \quad [5]$$

by the methods already outlined (1), we have immediately

$$\begin{aligned} \bar{F} &= A(e^{\Delta} - 1) - Bv + c_{11}(e^{\Delta} - 1)^2 \\ &\quad + c_{12}v(e^{\Delta} - 1) + c_{22}v^2 + \cdots \\ J &= C(e^{\Delta} - 1) + Av + d_{11}(e^{\Delta} - 1)^2 \\ &\quad + d_{12}v(e^{\Delta} - 1) + d_{22}v^2 + \cdots \end{aligned} \quad [6]$$

where

$$c_{11} = c'_{11} - (A/2), \qquad d_{11} = d'_{11} - (C/2). \quad [7]$$

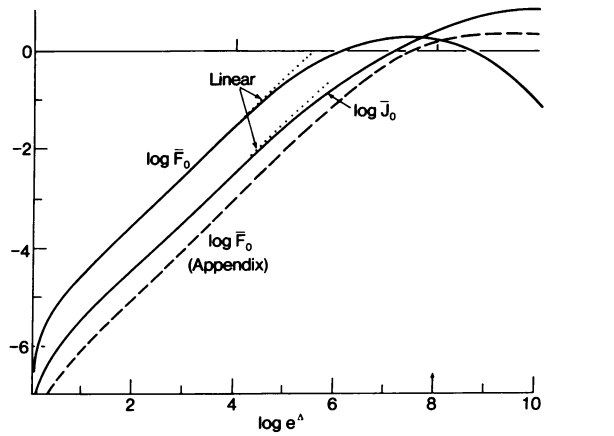

FIG. 4. Replot of $e^{\Delta_p} = 10^8$ case in Fig. 3 with a logarithmic ordinate. The *dotted curves* follow Eqs. 12.

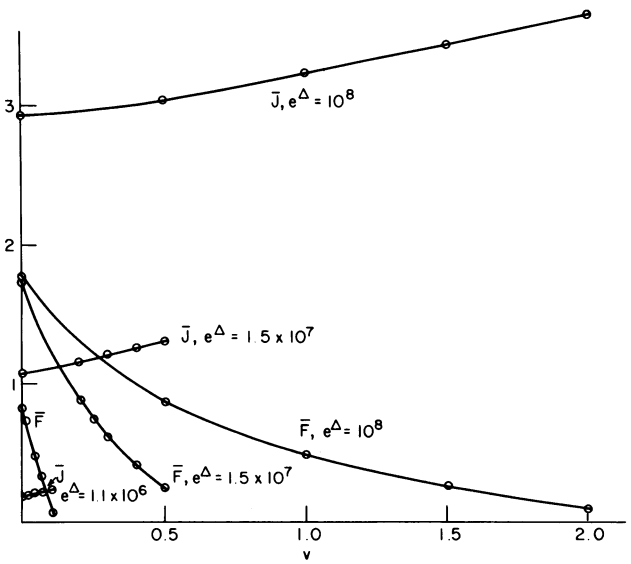

FIG. 5. Force-velocity and flux-velocity curves for several values of e^{Δ} (in the $e^{\Delta p} = 10^8$ case).

The physical significance of $e^{\Delta} - 1$ is that it is proportional to $c_T - c_T{}^e$, approximately, or to the corresponding activity difference, exactly.

Although the expansions in Eqs. **6** are valid in the $e^{\Delta p} = 100$ case (1), they do not provide any advantage over Eqs. **5**. But in the $e^{\Delta p} = 10^8$ case, the range (in Δ) of applicability is extended considerably by use of Eqs. **6**.

In the $e^{\Delta p} = 10^8$ case, we calculated the Δ, v linear and quadratic coefficients just as before (1), and then used Eqs. **7** to obtain

$$\bar{F} = 3.0177 \times 10^{-6}(e^{\Delta} - 1) - 15.173v - 2.35 \times 10^{-11}(e^{\Delta} - 1)^2 + 4.5498 \times 10^{-5}v(e^{\Delta} - 1) + 5.4296 \times 10^{-4}v^2 + \cdots \quad [8]$$

$$J = 3.6547 \times 10^{-7}(e^{\Delta} - 1) + 3.0177 \times 10^{-6}v - 1.28 \times 10^{-12}(e^{\Delta} - 1)^2 + 2.3066 \times 10^{-6}v(e^{\Delta} - 1) + 1.9403 \times 10^{-5}v^2 + \cdots \quad [9]$$

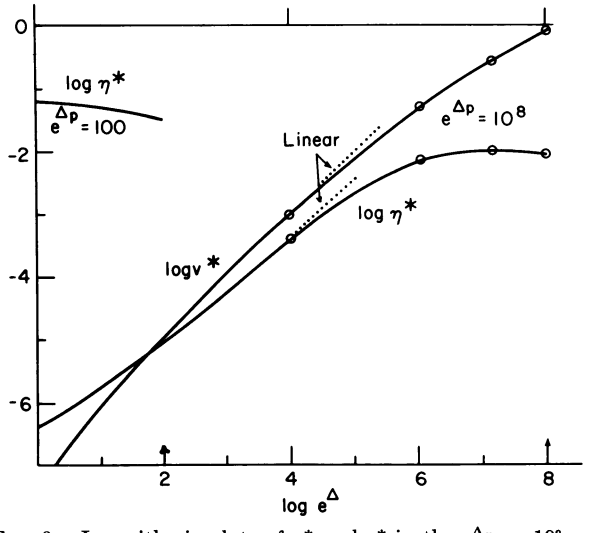

FIG. 6. Logarithmic plots of η^* and v^* in the $e^{\Delta p} = 10^8$ case and of η^* in the $e^{\Delta p} = 100$ case. The *dotted curves* follow Eqs. **13**.

The range in v of primary theoretical interest is $0 \leqslant v \leqslant v_{max}$. We can use the linear terms in Eq. **8** to obtain

$$v_{max} \cong 1.989 \times 10^{-7}(e^{\Delta} - 1). \quad [10]$$

If this value of v is substituted in Eq. **8**, we find that at, say, $e^{\Delta} = 10^3$, the two linear terms are about 130 times as large as the largest quadratic term (the v^2 term is negligible). Similarly, in Eq. **9**, at $e^{\Delta} = 10^3$ and $v \cong v_{max}$, the first term is about 285 times as large as the largest quadratic term (the v and v^2 terms are negligible). Thus, the approximation

$$\bar{F} = A(e^{\Delta} - 1) - Bv \qquad J = C(e^{\Delta} - 1) \quad [11]$$

is quite good at least to $e^{\Delta} = 10^3$.

On the scale of Fig. 4,

$$\bar{F}_0 = A(e^{\Delta} - 1), \quad J_0 = C(e^{\Delta} - 1) \quad [12]$$

are good approximations to about $e^{\Delta} = 10^4$ (the dotted "linear" curves in Fig. 4 follow Eqs. **12**).

Using $\eta = \bar{F}v/J\Delta$ and Eqs. **11**, we find easily the "linear" approximation

$$\eta^*(\Delta) = \eta^*(0)(e^{\Delta} - 1)/\Delta \qquad \eta^*(0) = A^2/4BC = 4.105 \times 10^{-7} \qquad v^*(\Delta) = (A/2B)(e^{\Delta} - 1) = v_{max}(\Delta)/2. \quad [13]$$

The solid curves for $e^{\Delta} < 10^4$ and the dotted curves for $e^{\Delta} > 10^4$ in Fig. 6 represent η^* and v^* from Eqs. **13**. The linear approximation is again satisfactory to $e^{\Delta} = 10^4$.

The efficiency at $e^{\Delta} = 10^8$ is larger than the efficiency at equilibrium, $\eta^*(0)$, by a factor of about 2.1×10^4. The extremely low efficiency at equilibrium is obviously (Eq. **13**) a consequence of the values of A, B, and C (see below).

An examination of the explicit integral expressions for the coefficients (1) clarifies the orders of magnitude found in the results quoted above. The very small quantity (in the $e^{\Delta p} = 10^8$ case) $\epsilon(x) \equiv g^e/\Sigma^e = 0(10^{-8})$ is crucial. The coefficients A and C are seen to be of order ϵ (the integrations over x have a significant effect, of course). B is of order unity. Hence if we take, say, $e^{\Delta} = 10^3$, v_{max}, Bv_{max}, Ae^{Δ}, and Ce^{Δ} are all of order $10^3\epsilon$, while Av_{max} is of order $10^3\epsilon^2$ (thus the v term in the J expansion, Eq. **6**, is negligible). Also, we observe (from the integrals) that c_{11} and d_{11} are of order ϵ^2, c_{12} and d_{12} are of order ϵ, while c_{22} and d_{22} are of order unity. The corresponding quadratic terms in Eqs. **6**, at v_{max} and $e^{\Delta} = 10^3$, are then all of order $10^6\epsilon^2$.

Results qualitatively similar to the above are presumably to be expected "near" equilibrium from most diagrams, in the realistic $e^{\Delta p} = 0(10^8)$ case. These "near" equilibrium properties are of no physiological interest but it is important, in at least one case, to examine the full e^{Δ} range and to establish the connection with irreversible thermodynamics (via A, B, and C).

As an addendum, we mention here one further result. Using Eqs. **5** and the derivatives $\partial\eta/\partial v$ and $\partial\eta/\partial\Delta$, one can obtain (after some algebra) an explicit general expression for the *slope* of $\eta^*(\Delta)$ at $\Delta = 0$:

$$\left(\frac{\partial\eta^*}{\partial\Delta}\right)_{\Delta=0} = a[(C + Aa)(c'_{11} + c_{12}a + c_{22}a^2) - (A - Ba)(d'_{11} + d_{12}a + d_{22}a^2)]/(C + Aa)^2 \quad [14]$$

where

$$a = (C/A)\{[1 + (A^2/BC)]^{1/2} - 1\}.$$

The value of $\eta^*(0)$ depends on A, B, and C only; the slope at $\Delta = 0$ depends on quadratic coefficients as well. The slope is negative in our $e^{\Delta p} = 100$ case and positive in the $e^{\Delta p} = 10^8$ case (see Fig. 6). In the latter case, Eq. **14** simplifies to

$$\left(\frac{\partial \eta^*}{\partial \Delta}\right)_{\Delta=0} \cong \frac{A^2}{8BC} \cong \frac{\eta^*(0)}{2}.$$

Rate of entropy production

As we have seen in our two examples with $e^{\Delta p} = 100$ and $e^{\Delta p} = 10^8$, the optimal efficiency $\eta^*(\Delta)$ does not have a maximum at $\Delta = 0$, as might have been expected intuitively; in fact, in the $e^{\Delta p} = 10^8$ case, $\eta^*(\Delta)$ *increases* considerably between $\Delta = 0$ and $e^{\Delta} = 10^8$ (and passes through a maximum on the way). These "odd" properties of η^* may be attributed to the fact that the fundamental *thermodynamic* quantity is the *difference* $T\dot{S}_i = J\Delta - \bar{F}v$ rather than the *quotient* $\eta = \bar{F}v/J\Delta$, where $\dot{S}_i$ is the rate of entropy production. Thus, $\dot{S}_i$ (Δ,v) has a minimum at equilibrium ($\dot{S}_i = 0$ when $\Delta = 0$, $v = 0$). Near equilibrium, $T\dot{S}_i = C\Delta^2 + Bv^2$. Along the line $v = 0$ in the Δ, v plane (isometric contractions), $\dot{S}_i(\Delta)$ presumably increases monotonically with Δ since, in the product $J_0\Delta$, $J_0(\Delta)$ presumably never decreases and Δ always increases. We say "presumably" because we do not have a general proof for an arbitrary diagram.

The related question arises as to whether $\dot{S}_i(v)$ has a minimum at $v = 0$ for an arbitrary fixed Δ. This is true near equilibrium, but it is easy to see that it is *not* true for an arbitrary Δ (even in the quadratic regime of Eqs. **5**). One might surmise that $\dot{S}_i(\Delta)$ increases monotonically along the curve $v^*(\Delta)$ in the Δ, v plane. This is the case in our $e^{\Delta p} = 100$ and $e^{\Delta p} = 10^8$ examples, but we have not proved that it is a general property (i.e., for any diagram).

APPENDIX

A simple model with qualitative properties similar to the above is one in which $g(x)$ is a step function at $x = 0$. Fig. 1 applies here and the notation is now *not* dimensionless. We use

$$f(x) = k_0 e^{-x^2/2\sigma^2}, \qquad f' = \text{constant} \qquad [15]$$

and

$$\begin{aligned} g(x) &= g^e e^{\Delta} \qquad (x < 0) \\ &= 0 \qquad (x > 0). \end{aligned} \qquad [16]$$

Then we must have

$$\begin{aligned} g'(x) &= k_0 e^{-x^2/2\sigma^2} g^e/f' \qquad (x < 0) \\ &= 0 \ (x > 0). \end{aligned} \qquad [17]$$

The force function is $F(x) = kTx/\sigma^2$. Ordinarily we take f' and $g^e e^{\Delta p}$ of order k_0, and $e^{\Delta p} = 0(10^8)$. In this case g' is very small.

One property that is easy to express in closed form is $\bar{F}_0(\Delta)$. Using $n_0 = (f + g')/(f + g' + f' + g)$, we find from

$$\bar{F}_0 = \frac{1}{d}\int_{-\infty}^{+\infty} n_0(x)F(x)dx \qquad [18]$$

that

$$\frac{\bar{F}_0 d}{kT} = \ln\left[\frac{\left(1 + \frac{f'}{k_0}\right)\left(1 + \frac{g^e e^{\Delta}}{f'}\right)}{\left(1 + \frac{f'}{k_0} + \frac{g^e}{f'} + \frac{g^e e^{\Delta}}{k_0}\right)}\right]. \qquad [19]$$

When $\Delta = 0$, this gives (as it should) $\bar{F}_0 = 0$. When $e^{\Delta} \to \infty$, we have

$$\bar{F}_0 d/kT \to \ln\left(1 + \frac{k_0}{f'}\right). \qquad [20]$$

As a numerical example, let us take

$$f' = 1, \qquad k_0 = 10$$

$$g^e e^{\Delta p} = 10^8 \, g^e = 10, \qquad g^e = 10^{-7}.$$

Then

$$\frac{\bar{F}_0 d}{kT} = \ln\left[\frac{1.1\ (1 + 10^{-7}e^{\Delta})}{(1.1 + 10^{-7} + 10^{-8}e^{\Delta})}\right] \qquad [21]$$

This function is included in Figs. 3 and 4 (*dashed line*).

1. Chen, Y. & Hill, T. L. (1974) *Proc. Nat. Acad. Sci. USA* **71**, 1982–1986.
2. Hill, T. L. (1975) in *Progress in Biophysics and Molecular Biology*, eds. Butler, J. A. V. & Noble, D. (Pergamon Press, New York), Vol. 29, in press.